

Journal of Materials Chemistry C

Accepted Manuscript



This is an *Accepted Manuscript*, which has been through the Royal Society of Chemistry peer review process and has been accepted for publication.

Accepted Manuscripts are published online shortly after acceptance, before technical editing, formatting and proof reading. Using this free service, authors can make their results available to the community, in citable form, before we publish the edited article. We will replace this *Accepted Manuscript* with the edited and formatted *Advance Article* as soon as it is available.

You can find more information about *Accepted Manuscripts* in the [Information for Authors](#).

Please note that technical editing may introduce minor changes to the text and/or graphics, which may alter content. The journal's standard [Terms & Conditions](#) and the [Ethical guidelines](#) still apply. In no event shall the Royal Society of Chemistry be held responsible for any errors or omissions in this *Accepted Manuscript* or any consequences arising from the use of any information it contains.

An Ultrafast Response Grating Structural ZnO Photodetector with Back-to-Back Schottky Barriers Produced by Hydrothermal Growth

*Cheolmin Park,^{a,b} Jihye Lee,^{a,b} Hye-Mi So,^b Won Seok Chang^{*a,b}*

^aNano-mechatronics Department, Korea University of Science and Technology (UST), 217 Gajeong-ro Yuseong-gu, Daejeon, 305-333, Korea

^bNano-convergence Mechanical System Research Division, Korea Institute of Machinery and Materials (KIMM), 156 Gajungbukno, Yuseong-gu, Daejeon, 305-343, Korea

KEYWORDS: zinc oxide, ultraviolet photodetector, nanoimprint lithography, hydrothermal growth, grating structure

ABSTRACT

An ultrafast response metal-semiconductor-metal type ZnO ultraviolet photodetector was fabricated by ultraviolet nanoimprint lithography (UV-NIL) with hydrothermal synthesis. The high performance of response time was caused by the Schottky barrier formation due to controlling growth time of hydrothermal synthesis and grating structure of ZnO produced by position-controlled patterning method of UV-NIL. With 2 kHz on/off frequency of ultraviolet light using optical chopper, the device exhibits a rising time of 43 μsec and a falling time of 54 μsec at low bias voltage (0.5 V) with a responsivity of 22.1 A/W in the active area of $5 \times 5 \mu\text{m}^2$. On the basis of comparing other fast response ZnO photodetectors, our device definitely presents easy and low-cost fabrication methods as well as high performance.

Introduction

Zinc oxide has attracted great interest regarding its use in various optoelectronics such as photon detectors,^{1,2} ultraviolet (UV) nanolasers^{3,4} and UV/blue LEDs (light-emitting diodes)^{5,6} due to its intrinsic properties such as a direct and wide band gap ($E_g = 3.4$ eV at room temperature) with a large exciton binding energy of 60 meV.⁷ With these properties, the nanostructure of ZnO improves the performance of ZnO UV photodetectors, such as high gain and fast response time due to the high surface-to-volume ratio.⁸ However, it is well known that the surface states of a ZnO nanostructure differ depending on its morphology and processing conditions during synthesis.⁹⁻¹¹ The main cause for this difference has been considered to be the formation of zinc interstitials (Zn_i) and oxygen vacancies (V_o) on the surface due to non-stoichiometry, inducing a polar character.^{9,12} The surface character affects not only the intrinsic properties of ZnO but also the electrical contact with the electrode in functional ZnO devices. Therefore, to obtain the desired surface condition, post-processing has been largely researched, including annealing^{13,14} and plasma treatments^{15,16}. However, the additional processes usually require a high-processing temperature and chamber equipment, which lead to disadvantages such as high costs, time-consuming processing, and limited device types.

In this study, without additional post-processing of nanostructured ZnO characteristics, we produced obvious Schottky barrier with Ti/Au electrodes through the controlled growth time of hydrothermal synthesis. By virtue of the method and the grating structure of ZnO due to ultraviolet-nanoimprint lithography (UV-NIL)^{17,18}, an ultrafast response metal-semiconductor-metal (MSM) type UV photodetector was achieved easily and cost-effectively. The moderate growth time for forming the Schottky barrier was identified by comparing distinctly different growth time in this paper to observe the barrier effect on the MSM type photodetector. The

surface states of ZnO due to those different growth times were evaluated using scanning electron microscopy (SEM), X-ray photoelectron spectroscopy (XPS) and macro photoluminescence (PL). In order to confirm the back-to-back Schottky barrier effect of MSM type photodetector comparing of ohmic-like junction, the optoelectric properties of photodetectors were studied using scanning photocurrent microscopy (SPCM), the current-voltage (I-V) characteristics under illumination with UV light and response time by an optical chopper.

Furthermore, although ZnO nanowire-based UV photodetectors have been researched largely in order to obtain high gain and fast response time, its results present disadvantages such as difficulty of control for fabrication, low-output current and high cost.^{17,19} For solving these problems, we considered the UV-NIL with controlled hydrothermal synthesis for fabricating position-controlled ZnO nanostructure with modulated surface state. Consequently, despite not having a nanowire and a complex heterojunction structure, our attempt firstly demonstrates an ultrafast rising time (43 μsec) and falling time (54 μsec) at a low bias voltage of 0.5 V in the active area of $5 \times 5 \mu\text{m}^2$, retaining its response current level and non-distorted current shape until 2 kHz of chopping frequency for UV light.

Experimental Section

Sample preparation The ZnO precursor resin for UV-NIL was prepared as following steps: 1) 0.5 mol zinc acetate dehydrate ($\text{Zn}(\text{CH}_3\text{COO})_2 \cdot 2\text{H}_2\text{O}$, Aldrich, Wyoming, IL, USA, 99.5%), the molar equivalent of monoethanolamine (MEA, $\text{NH}_2\text{CH}_2\text{CH}_2\text{OH}$, Aldrich, 99.5%), and 2-nitrobenzaldehyde (UV-Linker, Aldrich) were dissolved in 2-methoxyethanol (2ME ($\text{CH}_3\text{OCH}_2\text{CH}_2\text{OH}$, Aldrich, 99.5%), and 2) the resultant solution was stirred at 24°C for 3 h and at 75°C for 24 h in order to produce homogeneous solution. The ZnO nanoline pattern acting as a

seed for hydrothermal growth was deposited by UV-NIL with the ZnO precursor resin, which included the following steps. The ZnO precursor was spin-coated on the SiO₂/Si substrate at 3500 rpm for 1 min. Then, the sample was prebaked on a hot plate at 80°C. A polyurethane acrylate (PUA) mold with a line nanopattern with a 200 nm line width and 1 μm period was attached to the substrate, followed by illumination with UV light to cure the resin under an air pressure of 0.02 MPa to the mold. As a result, a ZnO thin film layer with line-nanopatterned ZnO remained on the substrate. Then, the sample was annealed in a furnace at 350°C for 1 h for crystallization to form the seed layer of sample A, B with the removal of organics. After the seed layer of sample B underwent wet etching with 0.25% HNO₃ solution, only the line-nanopatterned ZnO remained. Additionally, hydrothermal growth was achieved by immersing the substrates into the prepared solution at 70°C for 3 min for sample A and 20 min for sample B. Then, the substrates were rinsed with deionized water and dried by blowing N₂ gas. The prepared solution for the hydrothermal growth was (25 mM)-zinc nitrate hexahydrate (Zn(NO₃)₂ · 6H₂O, Aldrich, 98%) in aqueous water with (25 mM)-hexamethylenetetramine (C₆H₁₂N₄, Aldrich, 99.5%) and (0.834 mM)-polyethylenimine (PEI, Aldrich, molecular weight 1300 g/mol by LS). The MSM structure of the device was defined by photolithography and the lift-off process. The active area between electrodes was 5 × 5 μm², and the electrodes were deposited by Ti/Au (30 nm/300 nm) using the thermal evaporation method (KVE-T2000, Korea).

Characteristics The morphology of the fabricated grating structural ZnO on the SiO₂/Si substrate was investigated by scanning electron microscopy (S-4800, Hitachi). The surface chemical properties were analyzed by X-ray photoelectron spectroscopy (Kratos, Axis nova). The measured O1s and Zn2p_{3/2} peaks were deconvoluted using the OriginPro 8.6. The surface characteristics of the samples were also investigated by macro photoluminescence (PL) using a

spectrofluorometer (FluoroLog®-3, Horiba) in the spectral range of 330-750 nm with 0.35 nm resolution. The samples were positioned at 45° between the excitation light (295 nm wavelength) and the detector with a spot size of $1.5 \times 2 \text{ cm}^2$. The electric contact between the samples and electrodes was visually confirmed by spatially resolved photocurrent using scanning photocurrent microscopy (homemade). The area of $8 \times 8 \text{ }\mu\text{m}^2$ was scanned under a 405 nm light source with a 100× objective lens (NA 0.8). The dark and photogenerated current produced by a 355 nm laser were measured using a high-speed source/monitor unit (E5262A, Agilent Technologies) in a dark room. The fast response time under illumination of the UV laser chopped by an optical chopper (300CD, Scitec Instruments) was measured using a low-noise current preamplifier (SR570, Stanford Research Systems).

Results and Discussion

In the sample preparation, the grating structural ZnO seed layer was formed by UV-NIL and the thermal annealing of precursor resin (at 350°C for 1 h in a furnace). Though the line width in PUA mold was 200 nm, the resultant width in ZnO was shrunk due to crystallization and evaporation of organic components. Also, due to thermal annealing at high temperature, oxygen vacancies were generated in ZnO. After that, the seed layer of one sample (sample B) underwent wet etching for forming separated grating structure, while the other sample (sample A) didn't because of supplementing photocurrent level. The respectively resultant ZnO seed layers were hydrothermally synthesized using extremely different growth times (sample A: 3 min, sample B: 20 min) at 70°C in order to confirm the distinct growth time for forming Schottky barrier with Ti/Au electrodes. Fig. 1a and 1d present diagrams of sample A and B, respectively. The entire area on the SiO₂/Si substrate of sample A has a ZnO thin layer with grating structural ZnO on the

layer. Sample B only has thicker grating structural ZnO due to the longer growth time after wet etching on the surface. Fig. 1b, 1c, 1e and 1f present SEM images of samples A and B, respectively, which confirm the well-produced ZnO grating structure. The structure is intended to improve the fast response time in a MSM type photodetector by providing a directional current path. The X-ray diffraction (XRD) profiles of two samples show (100), (002), (101) reflections in Fig. S1 (Supporting Information), which indicates the wurzite crystal structure. Due to the different growth time, relative crystallinity of sample B is better than sample A, while sample A has very smaller grain size associated with high density of oxygen vacancies. The insets of Fig. 1c and 1f show expanded SEM images of the top view. The sample A has rough surface with grain size below 10 nm, while sample B shows randomly grown rods with diameter of 30~100 nm and hexagonal structure on the top surface. The hierarchically grown ZnO nanorods of sample B could have higher surface to volume ratio than sample A. Although the reason for existence of the ZnO thin layer in sample A is to supplement the current level compared with sample B, the surface state of sample A is uniform due to the hydrothermal synthesis of the entire sample area.

To evaluate the surface states of samples A and B, XPS was used, and the results are presented in Fig. 2a-c. The measured XPS spectra of O 1s peaks were deconvoluted into three peaks²⁰ using a combination of Gaussian (80%) and Lorentzian (20%) fits, as illustrated in Fig. 2a and 2b. The lower binding energy peak (LP) at 530 eV is related to the O-Zn bonds in the hexagonal wurzite ZnO structure. The medium binding energy peak (MP) at 531 eV is related to the oxygen vacancy that is due to adsorbed O²⁻ ions in the oxygen-deficient regions. Finally, the higher binding energy peak (HP) at 532 eV is associated with chemisorbed or dissociated oxygen and/or OH⁻ groups on the surface. Among these three peaks, the MP differs remarkably in the

two samples, revealing that sample A contains more oxygen vacancies than sample B. Correspondingly, Fig. 2c reveals that the Zn 2p_{3/2} peak of sample A shifted to a slightly higher binding energy than sample B. This shift could also be related to the abundance of oxygen vacancies inducing the lattice constant of zinc to shorten.²¹

To verify the XPS data, macro PL spectra of both samples were measured, as shown in Fig. 2d. The PL spectra of the samples have the typical form of ZnO PL as NBE (near-band-edge) emission and DLE (deep-level emission).²² In the figure, the green emission²³ related to oxygen vacancy on the surface was noticeably generated in sample A compared with sample B. The macro PL corresponding to the XPS data indicated that the two samples clearly have distinct surface states. We assumed that the distinguished surface states could be attributed to the growth times of the hydrothermal synthesis because oxygen vacancies decrease with increasing growth time.

To determine the effect of two surface states on the electrical contact condition between metal and semiconductor and the resultant contact condition on the performance of the photodetector, we fabricated MSM-type photodetectors using both samples. The critical factor of electric contact affecting the performance of a device could be the existence of a Schottky barrier because its presence strongly affects charge injection and extraction between metals and semiconductor. The existence of the barrier on both devices was confirmed by measuring the spatially resolved photocurrent using SPCM, as shown in Fig. 3a, 3d. The one-dimensional data of the white dashed line in the SPCM images are presented in Fig. 3b and 3e, and indicate that at the interface between the metal and n-type semiconducting ZnO, sample A has ohmic-like contact, while sample B has Schottky contact. The inset of Fig. 3e presents the band diagram of

the double Schottky junction in the MSM-type device. Under equal intensities of light, the different amount of photocurrent in the two samples could be attributed to the difference in the ZnO volume and surface-to-volume ratio due to structural effects. A small asymmetric amount of photocurrent at both side interfaces in sample B (Fig. 3e) is estimated because of subtly different surface states. The mechanism of dissimilar electrical contacts depending on the surface conditions can be indicated from the band diagram in Fig. 3c and 3f. The oxygen vacancies of ZnO play a role as donors because missing oxygen leaves free electrons.²⁴ At the interface, the abundant oxygen vacancies on the surface increase the Fermi level and the depletion width of Schottky barrier narrows, which causes carrier transfer as field emission and direct tunneling (Fig. 3c).²⁵ In contrast to sample A with ohmic-like contact, because sample B has a lower electron density on the surface than sample A, the relatively wide depletion width forces electrons to transfer over the barrier as the mechanism of thermionic emission (Fig. 3f).²⁵

The effect of distinct contact conditions on the fundamental performance of photodetectors was investigated by measuring the I - V characteristics under dark and UV light and the long time response with UV on/off control, as shown in Fig. 4. The dark current of sample A was much lower than 5 pA (Fig. 4a). And the dark current of sample B has the typical form of a double Schottky barrier (Fig. 4d).²⁶ At low bias voltage, the current increases sharply, which is due to the changing depletion width of the barrier.²⁶ Under illumination of UV light, sample A exhibits almost metallic conductivity by virtue of its ohmic-like junction (Fig. 4b), while sample B exhibits a symmetric nonlinear curve due to the back-to-back Schottky barrier (Fig. 4e). The long time response under on/off illumination of UV light was also distinguished, as illustrated in Fig. 4c and 4f. With UV light exposure, the photocurrent of sample A increases smoothly and is saturated. Upon turning off the UV light, the photocurrent decreases as a logarithmic function.

However, the photocurrent of sample B (Fig. 4f) increases sharply once the light turns on, followed by a gradual increase. Similarly, the photocurrent rapidly decreases upon turning off the light and then continued to decrease slowly. The sudden change of photocurrent is attributed to the Schottky barrier because of two factors: 1) the photo-generated electron-hole pairs are separated rapidly by the built-in electric field of the barriers and 2) the barriers altered due to changing of the interface state by desorption of oxygen ions.^{8,27} Those factors could abruptly affect the carrier transport. After the sudden change of the photocurrent when turning on the light, a slow increase of the current continues until reaching the equilibrium of the adsorption and desorption of oxygen ions on the surface according to the ambient oxygen density under the illumination of UV light.²⁷ When turning off the light, after the sudden decrease of the current, it decreases slowly until reaching the equilibrium under the dark. Therefore, in Fig. 4f, the red dashed lines indicate the effect of the Schottky barrier, while the green dashed lines are attributed to the surface state interacted with the ambient oxygen density.

The influence on Schottky barrier and surface state of the sample which has more growth time (40 min) than sample B (20 min) shows remarkably different optoelectric properties as comparing with sample B as shown in Fig. S2. In that case, the sample (growth time of 40 min) has a dominant influence of the high surface to volume ratio than the effect of Schottky barrier. In other words, it has higher gain and lower response time than sample B, which could be considered as two reasons: 1) generally, the gain has trade off relation with response time and 2) more randomly grown rods could form non-Schottky barriers with metal because of various energy levels at the junction due to more uneven contact conditions than sample B. Accordingly, the determination of moderate growth time could be important for a desired functional device. In our experiments, for achieving the fast response performance, the sample B is more adequate

than the sample with 40 min growth time. In addition, by the growth time, the amount of photocurrent according to the intensity levels of UV light alters because of the surface to volume ratio and the light trapping effect due to different structural effect as shown in the Fig. S3, which could be also another consideration for the desired UV photodetector.

The photosensitivity was measured using the formula $(I_{ph} - I_{dark})/I_{dark}$, where I_{ph} is the photocurrent under UV light and I_{dark} is the dark current. The photosensitivities of samples A and B with active areas of $5 \times 5 \mu\text{m}^2$ were 27713 and 760, respectively, at 5 V under illumination of 355 nm (1.315 μW). The high photosensitivity of sample A is due to its low dark current of 3.5 pA. Using the formula $R = (I_{ph} - I_{dark})/P_{area}Area$, the responsivity (R) was obtained. In this formula, P_{area} is the intensity of light and $Area$ is the active area of the photodetector. R of samples A and B is 0.074 and 101.8 A/W, respectively. To confirm the existence of gain, we calculated the gain using the following formula²⁸ and assuming $\eta = 1$ for simplification:

$$G = \frac{N_{electron}}{N_{photon}} = \frac{Rhc}{\eta q \lambda} = \frac{\tau}{\tau_t}$$

Gain (G) is defined as the ratio of the number of electrons collected per unit time ($N_{electron}$) and the number of photons absorbed per unit time (N_{photon}). In the above formula, q is the elementary charge, h is Planck's constant, c is the speed of light and λ is the incident wavelength. In the last term, τ is the carrier lifetime and τ_t is the carrier transit time, which means that high gain (> 1) can be obtained in our experiment if a photo-generated hole circulates with a fast transit time while some of electrons are captured in the trap for a long lifetime. The calculated gain of samples A and B is respectively 0.26 and 355.57 by the second term

($Rhc/\eta q\lambda$) of the formula, which indicates that sample B has high gain despite sample A containing an ohmic-like junction and plentiful oxygen vacancies that can trap free electrons on the surface. For the reason, we considered the surface-to-volume ratio, carrier transit time and changing the depletion width of Schottky barriers once illumination of UV light. Those three reasons are described as below. First, sample B contains numerous nanorods with high surface-to-volume ratios. The second reason is that the clearly separated ZnO grating structure of sample B could enhance the mobility of carrier due to one directional current path, compared with non-grating structure as a film layer (two-directional structure). Finally, under UV light, increasing Fermi-level due to photo-generated electron and the remained electron by desorption of oxygen on the surface could narrow the depletion width of Schottky barriers.^{29,30}

A fast response time to light is one of the essential factors for evaluating a photodetector. Using a mechanical chopper, as illustrated in Fig. 5a, we measured the fast response time of both devices at low bias voltage (0.5 V) with chopper frequencies of 500 Hz, 1000 Hz and 2000 Hz. At 500 Hz, sample A has a more distorted response current shape (Fig. 5b) than sample B (Fig. 5c). We estimated that the reason for this difference could be the capacitance effect in the device.^{31,32} Because the sample A has narrower depletion width of metal contact and more oxygen vacancies than sample B, it could have a larger capacitance than sample B. Another phenomenon resulting from its capacitance is that the response current level of sample A decrease with increasing chopper frequency (Fig. 5b and 5d). However, notably, the level of sample B does not decrease (Fig. 5c and 5d) until a chopper frequency of 2 kHz.

Fig. 5e shows the enlarged response current shape of sample B (back-to-back Schottky barriers ZnO UV photodetector) at a chopping frequency of 2 kHz. In the figure, when turning on the

light, the response current reaches the completely saturated current level (the top blue dashed line). The non-distorted response current has a very fast rising time (43 μsec) and falling time (54 μsec) based on 10%–90% of the current level between red dashed lines. Ultimately, the reason for the fast response time of sample B could be attributed to the back-to-back Schottky barriers resulting from modulated ZnO surface state and the grating structure providing a directional current path. From the comparison of the fast response time with other ZnO UV photodetectors exhibiting below several millisecond response times in Table 1³³⁻³⁵, our device has extremely faster response time. However, the on/off ratio is low as 10.04. As mentioned before, the gain (on/off ratio) has trade off relation with response time. Therefore, if we obtain an increased gain, the response time could be slowed. Furthermore, other ZnO devices in the Table 1 have a heterojunction and/or nanowire structure, which require high-cost and time-consuming fabrication, making it difficult to produce commercial devices. In contrast, our novel back-to-back Schottky barrier ZnO UV photodetector fabricated by UV-NIL with hydrothermal synthesis could provide the feasibility because the approach involves an easy, simple and low-cost method, additionally enables mass production via the roll-to-roll process.

Conclusion

In summary, we produced easily and low-costly an ultrafast response ZnO UV photodetector, which is attributed to the formation of Schottky barriers, without additional post-processing, due to the modulated growth time of hydrothermal synthesis, and the directional current path owing to the ZnO grating structure by position-controlled patterning method of UV-NIL. We believe that, to the best of our knowledge, by the fabrication of UV-NIL with hydrothermal synthesis, we

achieved firstly high performance of ZnO UV photodetector comparable with ZnO nanowire and/or complex heterojunction structural devices. Our report could encourage scientists and engineers for the high performance of optoelectrical devices fabricated by UV-NIL with hydrothermal synthesis.

AUTHOR INFORMATION

Corresponding Author

*W. S. Chang. E-mail: paul@kimm.re.kr

Acknowledgments

W.S.Chang acknowledges financial support received from the Global Frontier R&D Program by the Center for Advanced Soft Electronics funded by the National Research Foundation under the Ministry of Science, ICT and Future Planning (2014M3A6A5060950) and the Basic Research Fund of KIMM (SC1020, NK188C). J.Lee acknowledges financial support from the National Research Foundation of Korea under Grant No. 2009-0082527.

References

- 1 H. Kind, H. Yan, B. Messer, M. Law and P. Yang, *Adv. Mater.*, 2002, **14**, 158.
- 2 H. Chang, Z. Sun, K. Ho, F. Y, X. Tao, F. Yan, W. M. Kwok and Z. Zheng, *Nanoscale*, 2011, **3**, 258-264.
- 3 H. Zhou, M. Wissinger, J. Fallert, R. Hauschild, F. Stelzl, C. Klingshirn and H. Kalt, *Appl. Phys. Lett.*, 2007, **91**, 181112.
- 4 D. J. Gargas, M. C. Moore, A. Ni, S. W. Chang, Z. Zhang, S. L. Chuang, and P. Yang, *ACS nano*, 2010, **4**, 3270-3276.
- 5 J. H. Lim, C. K. Kang, K. K. Kim, I. K. Park, D. K. Hwang and S. J. Park, *Adv. Mater.*, 2006, **18**, 2720-2724.
- 6 X. M. Zhang, M. Y. Lu, Y. Zhang, L. J. Chen and Z. L. Wang, *Adv. Mater.*, 2009, **21**, 2767-2770.
- 7 D. C. Look, *Mater. Sci. Eng., B* 2001, **80**, 383-387.
- 8 C. Soci, A. Zhang, B. Xiang, S. A. Dayeh, D. P. R. Aplin, J. Park, X. Y. Bao, Y. H. Lo, and D. Wang, *Nano Lett.*, 2007, **7**, 1003-1009.
- 9 A. B. Djurišić and Y. H. Leung, *Small*, 2006, **2**, 944-961.
- 10 W. W. Lee, S. B. Kim, J. Yi, W. T. Nichols and W. I. Park, *J. Phys. Chem. C*, 2011, **116**, 456-460.
- 11 I. Shalish, H. Temkin and V. Narayanamurti, *Phys. Rev. B*, 2004, **69**, 245401_1-245401_4.

- 12 H. Endo, M. Sugibuchi, K. Takahashi, S. Goto, S. Sugimura, K. Hane and Y. Kashiwaba, *Appl. Phys. Lett.*, 2007, **90**, 121906.
- 13 H. S. Kang, J. S. Kang, J. W. Kim and S. Y. Lee, *J. Appl. Phys.*, 2004, **95**, 1246-1250.
- 14 Z. B. Fang, Z. J. Yan, Y. S. Tan, X. Q. Liu and Y. Y. Wang, *Appl. Surf. Sci.*, 2005, **241**, 303-308.
- 15 M. Liu and H. K. Kim, *Appl. Phys. Lett.*, 2004, **84**, 173-175.
- 16 J. Zhang, H. Yang, Q. L. Zhang, S. Dong and J. K. Luo, *Appl. Surf. Sci.*, 2013, **282**, 390-395.
- 17 H. H. Park, X. Zhang, K. W. Lee, K. H. Kim, S. H. Jung, D. S. Park, Y. S. Choi, H. B. Shin, H. K. Sung, K. H. Park, H. K. Kang, H. H. Park and C. K. Ko, *CrystEngComm*, 2013, **15**, 3463-3469.
- 18 E. Chong, S. Kim, J. H. Choi, D. G. Choi, J. Y. Jung, J. H. Jeong, E. S. Lee, J. Lee, I. Park and J. Lee, *Nanoscale Res. Lett.*, 2014, **9**, 428.
- 19 N. S. Liu, G. J. Fang, W. Zeng, H. Zhou, F. Cheng, Q. Zheng, L. Y. Yuan, X. Zou and X. Z. Zhao, *ACS Appl. Mater. Interfaces*, 2010, **2**, 1973-1979.
- 20 S. Bang, S. Lee, Y. Ko, J. Park, S. Shin, H. Seo, and H. Jeon, *Nanoscale Res. Lett.*, 2012, **7**, 1-11.
- 21 S. Bang, S. Lee, J. Park, S. Park, Y. Ko, C. Choi, H. Chang, H. Park, H. Jeon, *Thin Solid Films*, 2011, **519**, 8109-8113.

- 22 P. Yang, H. Yan, S. Mao, R. Russo, J. Johnson, R. Saykally, N. Morris, J. Pham, R. He, H. J. Choi, *Adv. Funct. Mater.*, 2002, **12**, 323.
- 23 Y. Gong, T. Andelman, G. F. Neumark, S. O'Brien, and I. L. Kuskovsky, *Nanoscale Res. Lett.*, 2007, **2**, 297-302.
- 24 J. D. Hwang, Y. L. Lin and C. Y. Kung, *Nanotechnology*, 2013, **24**, 115709.
- 25 L. J. Brillson and Y. Lu, *J. Appl. Phys.*, 2011, **109**, 121301.
- 26 C. Van Opdorp and H. K. J. Kanerva, *Solid-State Electron.*, 1967, **10**, 401-421.
- 27 Q. H. Li, T. Gao, Y. G. Wang, and T. H. Wang, *Appl. Phys. Lett.*, 2005, **86**, 123117.
- 28 K. W. Liu, J. G. Ma, J. Y. Zhang, Y. M. Lu, D. Y. Jiang, B. H. Li, D. X. Zhao, Z. Z. Zhang, B. Yao, D. Z. Shen, *Solid-State Electron.*, 2007, **51**, 757-761.
- 29 F. Yi, Y. Huang, Z. Zhang, Q. Zhang and Y. Zhang, *Opt. Mater.*, 2013, **35**, 1532-1537.
- 30 Y. Hu, J. Zhou, P. H. Yeh, Z. Li, T. Y. Wei and Z. L. Wang, *Adv. Mat.*, 2010, **22**, 3327-3332.
- 31 J. Suehiro, N. Nakagawa, S. I. Hidaka, M. Ueda, K. Imasaka, M. Higashihata, T. Okada and M. Hara, *Nanotechnology*, 2006, **17**, 2567.
- 32 G. Xue, X. Yu, T. Yu, C. Bao, J. Zhang, J. Guan, H. Huang, Z. Tang, Z. Zou, *J. Phys. D: Appl. Phys.*, 2012, **45**, 425104.
- 33 Y. Q. Bie, Z. M. Liao, H. Z. Zhang, G. R. Li, Y. Ye, Y. B. Zhou, J. Xu, Z. X. Qin, L. Dai and D. P. Yu, *Adv. Mat.*, 2011, **23**, 649-653.
- 34 J. B. K. Law, J. T. L. Thong, *Appl. Phys. Lett.*, 2006, **88**, 133114.

35 B. Nie, J. G. Hu, L. B. Luo, C. Xie, L. H. Zeng, P. Lv, F. Z. Li, J. S. Jie, M. Feng, C. Y. Wu, Y. Q. Yu and S. H. Yu, *Small*, 2013, **9**, 2872-2879.

Figures

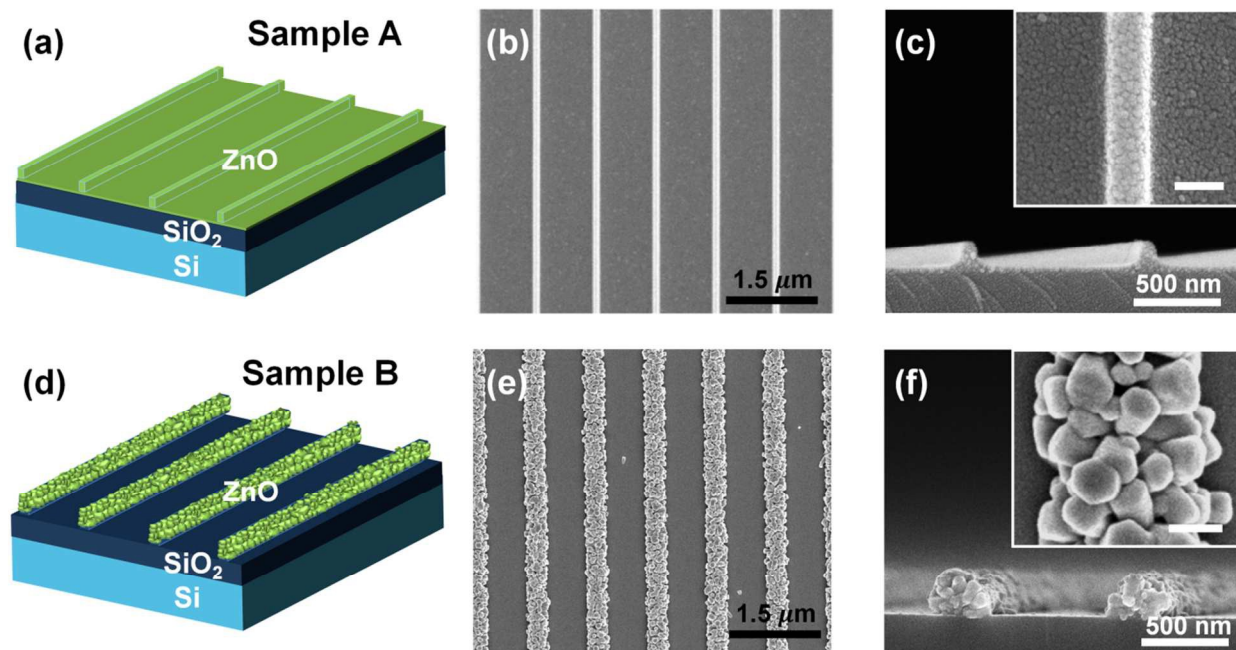


Fig. 1 Schematic illustrations of sample A (a) and B (b) on SiO₂/Si substrates. SEM images of sample A (b, c) and B (e, f). The top views of samples (b, e) show the ZnO grating structure with 1 μm period. Cross-sectional view of sample A (c) and B (f). The inset shows the top view of the expanded SEM images with a 100 nm scale bar.

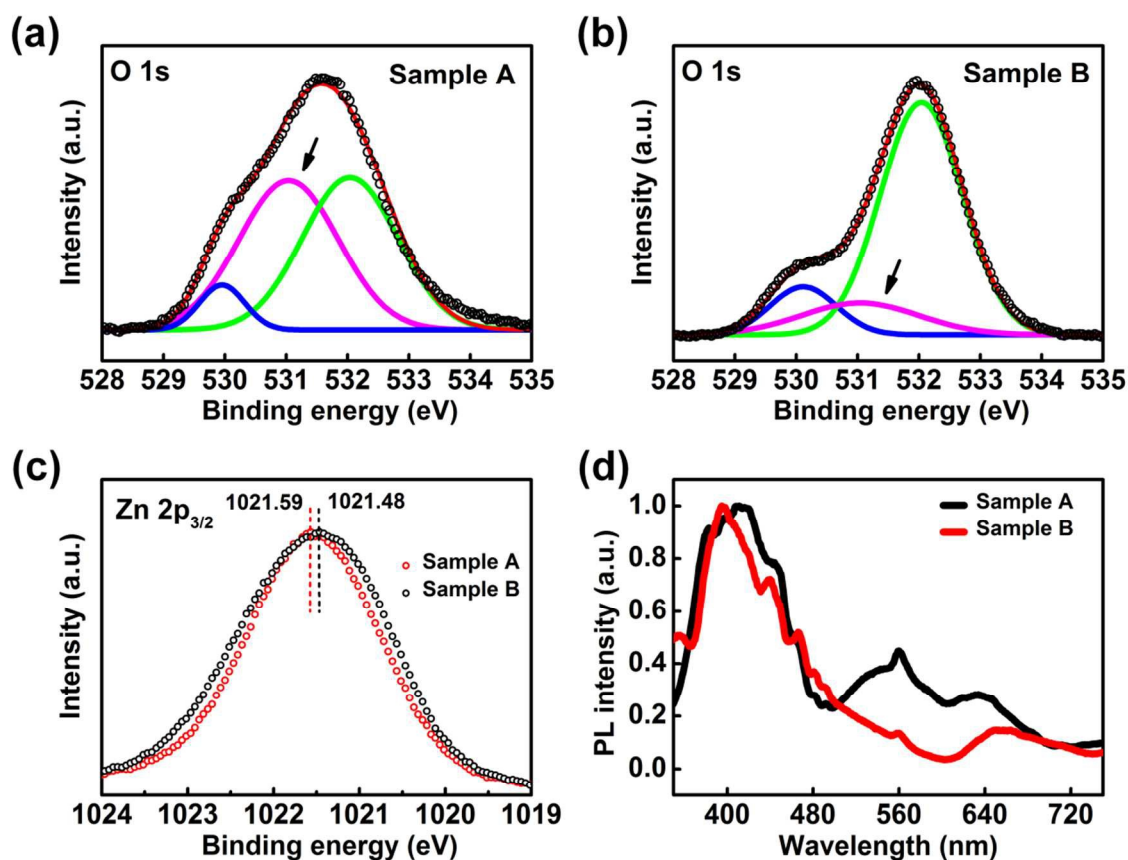


Fig. 2 (a, b and c) XPS data for samples A and B. (a, b) The O 1s peaks were deconvoluted to LP (blue), MP (purple) and HP (green). (c) Zn 2p_{3/2} peaks of samples A and B. (d) Macro PL spectra of samples A and B.

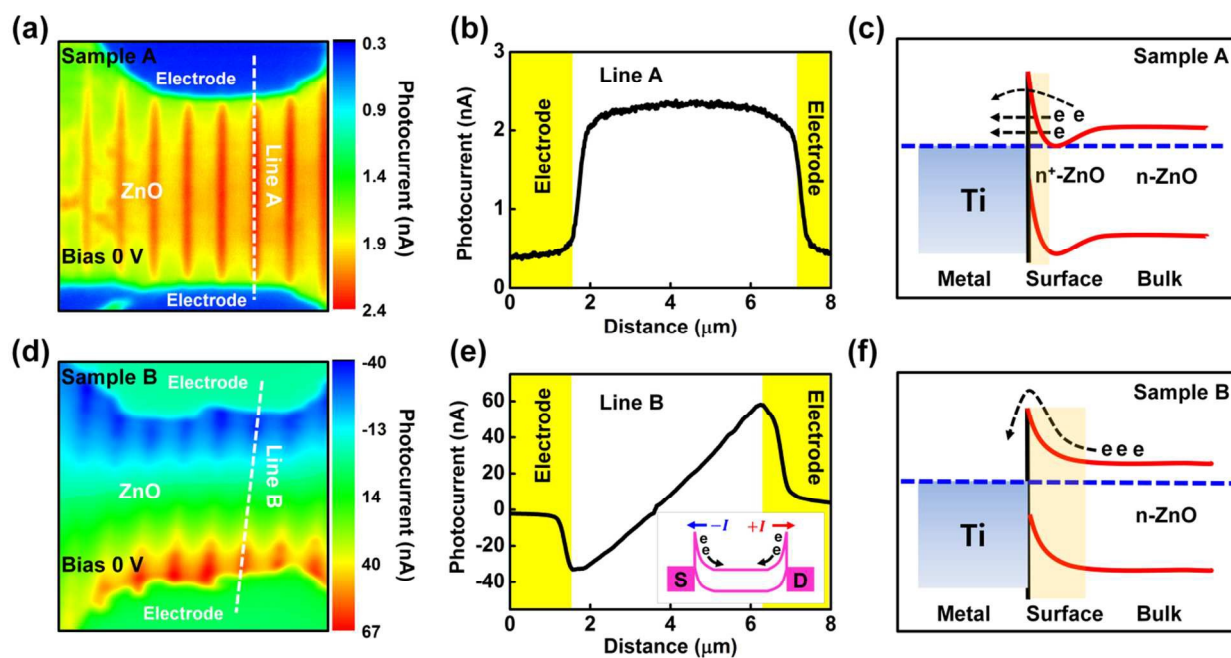


Fig. 3 (a, d) Spatially resolved photocurrent images of samples A and B. (b, e) The white dashed line in (a) and (d) indicates the one-dimensional photocurrent. The inset of (e) shows the band diagram of the double Schottky barrier in the MSM-type device. (c, f) Band diagrams of the interface between Ti metal and n-type semiconducting ZnO.

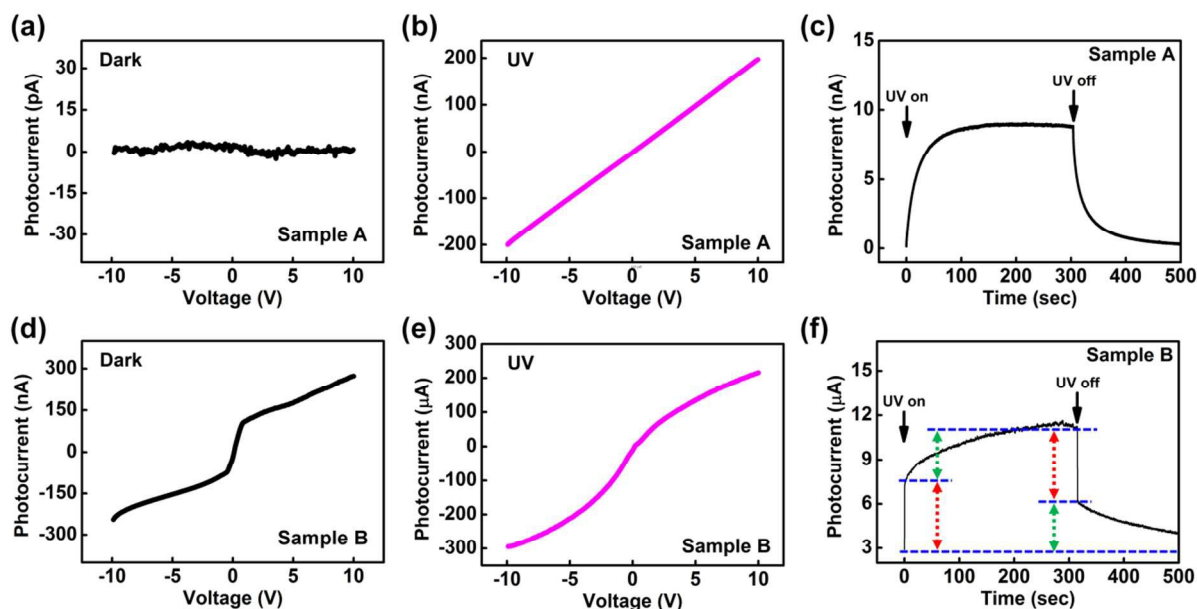


Fig. 4 Current-voltage characteristics of samples A and B in the dark (a, d) and under illumination with a 355 nm laser at an intensity of 2.4 mW (b, e). (c, f) Long time response of samples A and B at 2 V bias voltage for the on/off condition of UV light. The red dashed arrows indicate the Schottky effect, while the green dashed arrows show the effect of adsorption and desorption in (f).

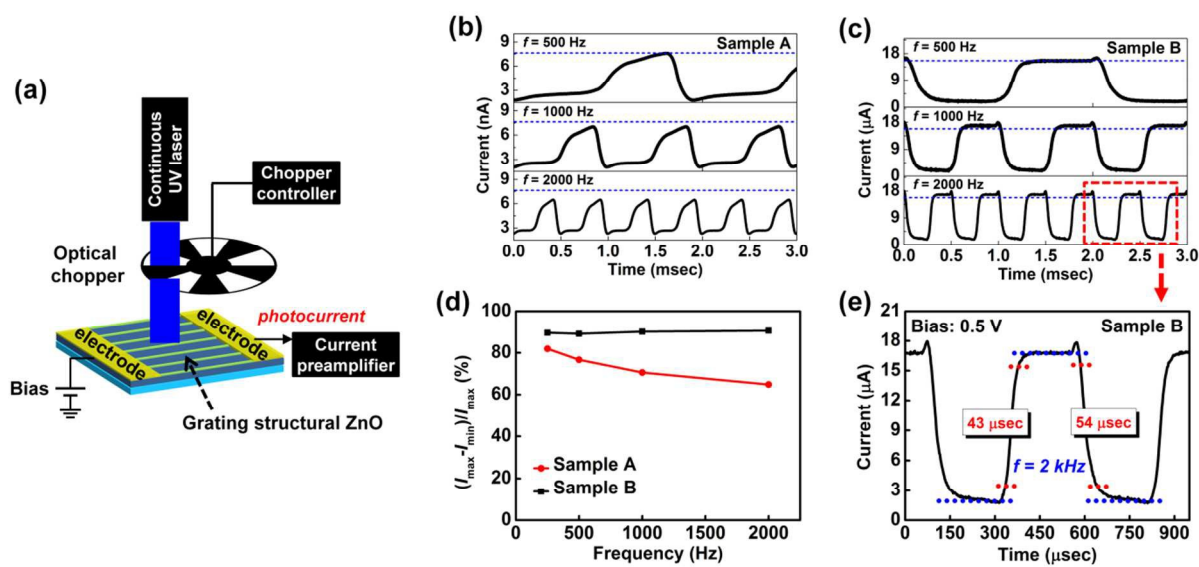
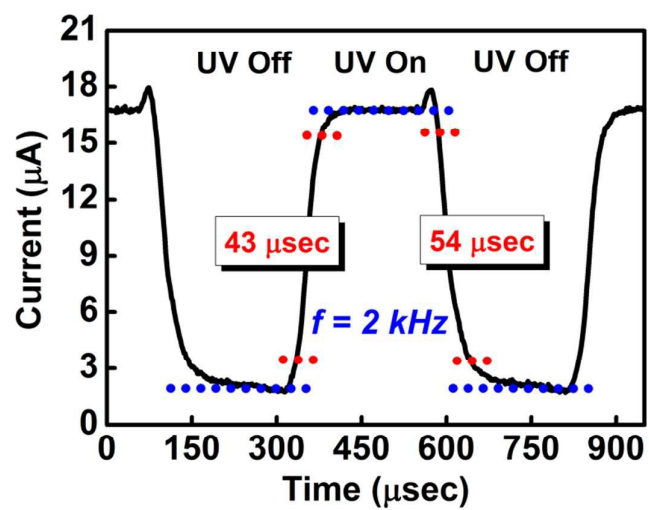
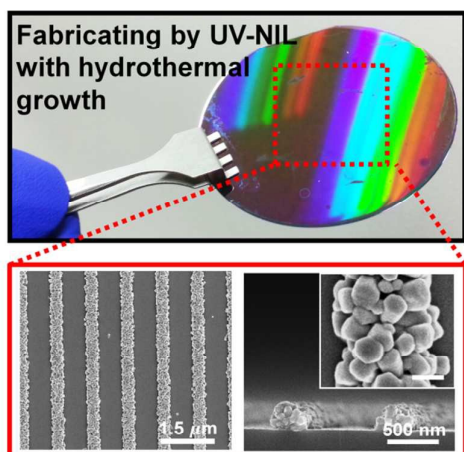


Fig. 5 (a) Schematic illumination of fast response time measurement and the MSM type grating structural ZnO photodetector. (b, c) Response of samples A and B at 0.5 V bias voltage under 355 nm laser illumination (4.9 mW) with chopping frequencies of 500, 1000, and 2000 Hz. (d) $(I_{max} - I_{min})/I_{max}$ based on the chopper frequency. (e) Expanded graph of (c) from 140 to 700 μs.

Table 1. Summary of ZnO UV photodetectors with rising and falling times of less than several milliseconds.

Materials	Device structure	Wavelength (nm)	t_r (ms)	t_f (ms)	R (A/W)	G	Ref
ZnO NRs grating structure	M-S-M (Schottky)	355	0.043	0.054	22.1	77.2	This work
ZnO/GaN nanowire	P-N junction	325	0.02	0.22	-	-	33
ZnO nanowires	M-S-M (Schottky)	370	0.2	0.3	-	-	34
Graphene/ZnO NR array	Schottky junction	365	0.7	3.6	113	385	35

TOC Graphics and Summary:



“Nanostructured ZnO UV photodetector produced by UV-NIL with hydrothermal growth achieved ultrafast response time.”